Supporting information

CO_2 Photoreduction by Formate Dehydrogenase and a Ru-complex in a Nanoporous Glass Reactor

Tomoyasu Noji,*[a] Tetsuro Jin,[b] Mamoru Nango,[a,c] Nobuo Kamiya[a] and Yutaka Amao[a]

[a] The OCU Advanced Research Institute for Natural Science & Technology (OCARINA), Osaka City University, 3-3-138 Sugimoto, Sumiyoshi-ku, Osaka 558-8585, Japan, E-mail: tnoji@ocarina.osaka-cu.ac.jp, TEL: +8152-735-3486

[b] Inorganic Functional Materials Research Institute, National Institute of Advanced Industrial Science and Technology (AIST), 1-8-31, Midorigaoka, Ikeda, Osaka 563-8577, Japan

[c] Monozukuri research center, Nagoya Institute of Technology, Gokiso-cho, Showa-ku, Nagoya 466-8555, Japan

*Corresponding Authors: tnoji@ocarina.osaka-cu.ac.jp (T.N.)

Abbreviations

ADH : alcohol dehydrogenase, AldDH : aldehyde dehydrogenase, FDH : formate dehydrogenase, MV^{2+} : methyl viologen, $MV^{\bullet+}$: the reduced form of methyl viologen, PGP50 : porous glass plate with nanopores of 50-nm, Rh-FDH : rhodamine-labelled formate dehydrogenase, $Ru(bpy)_3^{2+}$: tris(bipyridine)ruthenium(II), $Ru(bpy)_3/MV^{2+}$ solution : a solution containing $Ru(bpy)_3^{2+}$and MV^{2+}, $Ru(bpy)_3/MV^{2+}$/FDH solution : a solution containing $Ru(bpy)_3^{2+}$, MV^{2+}, and FDH, $Ru(bpy)_3/MV^{2+}$/PGP50 : PGP50 adsorbed $Ru(bpy)_3^{2+}$and MV^{2+} in the nanopores, $Ru(bpy)_3/MV^{2+}$/hydrogenase/PGP50 : PGP50 adsorbed $Ru(bpy)_3^{2+}$, MV^{2+}, and hydrogenase in the nanopores, $Ru(bpy)_3^{2+}/MV^{2+}$/FDH/PGP50 : PGP50 adsorbed $Ru(bpy)_3^{2+}$, MV^{2+}, and FDH in the nanopores

Materials and methods

Preparation of PGP. PGPs with dimensions of 1 mm × 4 cm × 4 cm and an average inner pore diameter of 50 nm (PGP50) were synthesized by acid leaching of phase-separated borosilicate glass.[1,2] The mother glass with a composition of $62.5SiO_2$-$28.3B_2O_3$-$9.2Na_2O$ (wt%) was first melted in a platinum crucible and then heated at 610 °C for 32 h for phase separation. The phase-separated glass was then leached in 1 N sulfuric acid at 90 °C for 2 days. The pore diameter, pore volume, and surface area of PGP50 were estimated by mercury penetration methods.[1,2] Pore volume,

and area receiving sunlight per unit weight of PGP50 were 0.323 cm^3/g and 9.7 cm^2/g, respectively.

Preparation of $Ru(bpy)_3^{2+}/MV^{2+}$/formate dehydrogenase-immobilized PGP50 ($Ru(bpy)_3^{2+}/MV^{2+}$/FDH/PGP50). FDH from *Candida boidinii* was purchased (0.4 U/mg lyophilizate, 3 U/mg protein, Roche Life Science). Mole concentration of FDH was calculated by assuming that all protein in lyophilizate is FDH. A PGP50 substrate (thickness: 1.0 mm) was immersed in a formate dehydrogenase (FDH)-containing medium (41 μM FDH in 25 mM MES-NaOH (pH 6.6)) at 4 °C for 24 h. The amount of FDH adsorbed in PGP50 was determined from the decrease in the absorbance of the soaking solution at 280 nm using a spectrophotometer (UV-1800, Shimadzu, Kyoto, Japan) (Figure S1). The resulting FDH immobilized-PGP50 was then immersed in medium A (0.1 M MES-NaOH (pH 6.6) and 20 mM EDTA·2Na) containing 0.5 mM $Ru(bpy)_3^{2+}$ and 3 mM MV^{2+} at 4 °C for 24 h. The amounts of $Ru(bpy)_3^{2+}$ and MV^{2+} adsorbed onto the PGP substrate were determined from the decrease in the absorbance of $Ru(bpy)_3^{2+}$ and MV^{2+} in the soaking solution according to a previously reported method.[3] The resulting $Ru(bpy)_3^{2+}/MV^{2+}$/FDH/PGP50 was rinsed with medium A.

Light-induced formic acid production assay. The total volume of the reaction cell for $Ru(bpy)_3^{2+}/MV^{2+}$/FDH/PGP50 (thickness: 1.0 mm) was 4.5 mL. The outer medium surrounding $Ru(bpy)_3^{2+}/MV^{2+}$/FDH/PGP50 was composed of medium B (0.1 M

MES-NaOH (pH 6.6), 20 mM EDTA·2Na, and 24 mM $NaHCO_3$). The volume of the outer medium was adjusted to 4.3 mL. A 64 mg fragment of $Ru(bpy)_3^{2+}/MV^{2+}$/FDH/PGP50 was put into the reaction cell. In the case of $Ru(bpy)_3^{2+}$, MV^{2+}, and FDH in solution ($Ru(bpy)_3^{2+}/MV^{2+}$/FDH solution), the reaction medium composition was medium B containing 0.5 mM $Ru(bpy)_3^{2+}$, 3 mM MV^{2+}, and 41 μM FDH. The $Ru(bpy)_3^{2+}/MV^{2+}$/FDH solution (0.65 mL) was put in a quartz cell with a 2 mm path length. $Ru(bpy)_3^{2+}/MV^{2+}$/FDH/PGP50 and the $Ru(bpy)_3^{2+}/MV^{2+}$/FDH solution were irradiated using a solar simulator (YSS-E40, Yamasita Denso, Tokyo, Japan) with stirring of the outer medium and $Ru(bpy)_3^{2+}/MV^{2+}$/FDH solution. The density of the photon flux generated by the solar simulator was measured in the wavelength range of 400−700 nm using a spectrometer (SILVER-Nova, 1 nm resolution, StellarNet, Tampa, FL, USA). The spectroradiometric calibration of the spectrometer was carried out at the time of factory shipment. From the reaction cell, 40–300 μL of solution was collected using a pipette, then diluted 10–20 times with Milli-Q water. The resulting solution was analyzed using an ion chromatography system (Dionex ICS-1100, Thermo Scientific, Waltham, MA, USA). The formic acid concentration was calibrated in advance. The rates of formic acid production/area (μmol HCOOH/(m^2·s)) were calculated from the light-receiving areas of 3.25 cm^2 for the solution system (0.65 mL solution) and 9.7 cm^2/g for the 1.0 mm thick PGP50 system. The light-induced formic acid production of $Ru(bpy)_3^{2+}/MV^{2+}$-immobilized PGP50 ($Ru(bpy)_3^{2+}/MV^{2+}$/PGP50) and a solution containing $Ru(bpy)_3^{2+}$ and MV^{2+} ($Ru(bpy)_3^{2+}/MV^{2+}$ solution) without FDH were also estimated using the same procedure. In Figure 2 in main text, the light-induced formic acid production per unit of light-receiving area of $Ru(bpy)_3^{2+}/MV^{2+}$/FDH/PGP50 and

the $Ru(bpy)_3^{2+}/MV^{2+}$/FDH solution were corrected by approximately 0.5 μmol HCOOH/(m^2·s), corresponding to the production observed for both $Ru(bpy)_3^{2+}/MV^{2+}$/PGP50 and the $Ru(bpy)_3^{2+}/MV^{2+}$ solution. The conversion efficiency from photon to formic acid was evaluated as 2 × [formic acid production rate (μmol HCOOH/(m^2·s))]/[photon flux density (μmol/(m^2·s))]. The photon flux density within the wavelength range of 400–700 nm was 1300 μmol/(m^2·s).

Preparation of rhodamine-labelled formate dehydrogenase (Rh-FDH). The FDH buffer solution (MES-NaOH buffer, 25 mM, pH 6.6) was replaced with a phosphate buffer solution (0.1 M, pH 7.2) containing 0.15 M NaCl by use of an ultrafiltration membrane (Amicon, 30 kDa-cutoff, Millipore, Billerica, MA, USA) to obtain 11 μM FDH. NHS-rhodamine (Thermo Scientific, Waltham, MA, USA) was dissolved in this solution, and the final FDH and NHS-rhodamine concentrations were adjusted to 5.4 and 55 μM, respectively. The solution was allowed to react in an ice bath for 12 h under dark conditions. Unreacted compounds were removed with a micro bio-spin column (Bio-Rad, Hercules, CA, USA). The conjugation ratio (rhodamine/FDH) was estimated to be 0.30 from the absorbance at 280 and 555 nm.

Preparation of rhodamine-FDH-immobilized PGP50. A PGP50 substrate (thickness: 1.0 mm) was immersed in an Rh-FDH-containing medium (6.0 μM Rh-FDH, 25 mM MES-NaOH, pH 6.6) at 4 °C for 24 h. The amount of Rh-FDH adsorbed onto PGP50

was determined from the decrease in the absorbance of the soaking solution at 555 nm using a spectrophotometer (UV-1800, Shimadzu, Kyoto, Japan).

Confocal laser scanning microscopy. Fluorescence imaging of the emission from Rh-FDH immobilised in PGP50 nanopores was performed using a confocal laser scanning microscope (NX-3DFLIM-N03, Tokyo Instruments, Tokyo, Japan) equipped with an objective lens (LUCPLFLN ×20; numerical aperture = 0.45, Olympus, Tokyo, Japan) and a CCD detector (DV420A-BEX2-DD, Andor Technology, Tokyo, Japan). A 532 nm semiconductor laser (J050GS-11; Showa Optronics Co., Ltd., Tokyo, Japan) was used as the excitation source. Using a laser intensity of 8.6 μW, a cross-section of PGP50 was observed to detect emissions from Rh-FDH at 563–661 nm. The XY images were obtained with a unit pixel size of 0.25 μm × 0.25 μm and a typical accumulation time of 0.01 s for each pixel.

The accumulation rate of formic acid in the nanopores inside PGP50.

[Production rate of formic acid per unit of light-receiving area (μmol HCOOH/(m^2·s))] × 3600/10000 × [light-receiving area per unit weight of PGP50 (cm^2/g PGP50)] / [pore volume per unit weight of PGP50 (cm^3/g PGP50)] = 1.4 × 3600/10000 × 9.7/0.323 = 15 mM HCOOH/h

The accumulation rate of formic acid in the $Ru(bpy)_3^{2+}/MV^{2+}$/FDH solution.

[Production rate of formic acid per unit of light-receiving area (μmol HCOOH/(m^2·s))] / [light pass length (cm)] × 3600/10000 = 0.10/0.2 × 3600/10000 = 0.18 mM HCOOH/h

The accumulation rate of $MV^{\bullet+}$ per unit of light-receiving area of $Ru(bpy)_3^{2+}/MV^{2+}$/PGP50. The photon flux density of a solar simulator (YSS-E40, Yamasita Denso, Tokyo, Japan) within 400–700 nm was 1300 μmol/(m^2·s) using a sensitivity corrected spectrometer (SILVER-Nova, StellarNet, Tampa, FL, USA). Blue trace in Figure S4 shows the photon flux density spectrum of a solar simulator. Black and red traces in Figure S4 show the transmittance spectra of PGP50 and $Ru(bpy)_3^{2+}/MV^{2+}$/PGP50 immersed in a solution, respectively (These spectra is referred from supprimentaly information in Ref.3). A green trace in Figure S4 shows a spectrum of photon flux density absorbed by $Ru(bpy)_3^{2+}/MV^{2+}$/PGP50, and equals to ([Transmittance spectra of PGP50 (%)] – [Transmittance spectra of $Ru(bpy)_3^{2+}/MV^{2+}$/PGP50 (%)]) × [Photon flux density of a solar simulator (μmol/(m^2·s))] /100. The photon flux density absorbed by $Ru(bpy)_3^{2+}/MV^{2+}$/PGP50 was 430 μmol/(m^2·s) in the range of 400–700 nm, correspond to 33% of the photon flux density of a solar simulator. The efficiency of the MV^{2+}-photoreduction estimated from the number of photons absorbed by $Ru(bpy)_3^{2+}$ in $Ru(bpy)_3^{2+}/MV^{2+}$/PGP50 (thickness: 1.0 mm) was about 3% under aerobic conditions.[3] The accumulation rate of $MV^{\bullet+}$ per

unit of light-receiving area of $Ru(bpy)_3^{2+}/MV^{2+}$/PGP50 was evaluated as 3/100 × [The photon flux density absorbed by $Ru(bpy)_3^{2+}/MV^{2+}$/PGP50 (μmol/(m^2·s))] = 3/100 ×430 = 13 μmol $MV^{\bullet+}$/(m^2·s) .

The conversion efficiency of $MV^{\bullet+}$ production in $Ru(bpy)_3^{2+}/MV^{2+}$/PGP50

[Rate of reduction of MV^{2+} per area (μmol/(m^2·s))] / [Photon flux density of a solar simulator (μmol/(m^2·s))] × 100 = 13/1300 × 100 = 1%.

The conversion efficiency from $MV^{\bullet+}$ to formic acid in nanopores inside PGP50.

[Rate of formic acid production per area (μmol/(m^2·s))] / [rate of reduction of MV^{2+} per area (μmol/(m^2·s))] × 2 × 100 = 1.4/13 × 2 × 100 = 22 %.

The conversion efficiency from $MV^{\bullet+}$ to formic acid in the $Ru(bpy)_3^{2+}/MV^{2+}$/FDH solution.

The conversion efficiency of the MV^{2+}-photoreduction of the $Ru(bpy)_3^{2+}/MV^{2+}$ solution per the photon flux density of a solar simulator within the wavelength range of 400-700 nm is about 1.5% under aerobic conditions.[3] The accumulation rate of $MV^{\bullet+}$ per unit of light-receiving area of the $Ru(bpy)_3^{2+}/MV^{2+}$ solution was evaluated as 1.5/100 ×

[Photon flux density of a solar simulator (μmol/(m^2·s))] = 1.5/100 × 1300 = 20 μmol $MV^{\bullet+}$/(m^2·s) . The conversion efficiency from $MV^{\bullet+}$ to formic acid evaluated as 2 × 100 × [rate of formic acid production per area (μmol/(m^2·s))] / [rate of reduction of MV^{2+} per area (μmol/(m^2·s))] = 2 × 100 × 0.1/20 = 1 %.

The accumulation rate of $MV^{\bullet+}$ concentration in the nanocavity inside PGP50.

[Accumulation rate of $MV^{\bullet+}$ per unit of light-receiving area (μmol $MV^{\bullet+}$/(m^2·s))] × 3600/10000 × [light-receiving area per unit weight of PGP50 (cm^2/g PGP50)] / [pore volume per unit weight of PGP50 (cm^3/g PGP50)] = 13 × 3600/10000 × 9.7/0.323 = 140 mM $MV^{\bullet+}$/h

The accumulation rate of $MV^{\bullet+}$ concentration in the the $Ru(bpy)_3^{2+}/MV^{2+}$ solution.

[Rate of formic acid production per area (μmol/(m^2·s))] / [light pass length (cm)] ×3600/10000 = 20/0.2 × 3600/10000 = 36 mM $MV^{\bullet+}$/h.

Physical appearance concentration of $Ru(bpy)_3^{2+}$ in $Ru(bpy)_3^{2+}/MV^{2+}$/FDH/PGP50 and the effective light-pass length of PGP50

Physical appearance concentration of $Ru(bpy)_3^{2+}$ in $Ru(bpy)_3^{2+}/MV^{2+}$/FDH/PGP50 is calculated by the amount of $Ru(bpy)_3^{2+}$ per unit of light-receiving area of PGP50 (0.31 μmol/cm^2) and the thickness of PGP50 (1 mm).

(0.31μmol/cm^2) / (1 mm) = 3.1 mM

The effective light-pass length of PGP50 is calculated using $Ru(bpy)_3^{2+}$ per unit of light-receiving area of PGP50 of 0.31 μmol/cm^2, physical appearance concentration in PGP50 system of 3.1 mM, and the concentration in nanopores of 9.3 mM.

0.31 μmol/cm^2 = 3.1 mM × 1 mm = 9.3 mM × 0.33 mm.

The value of 0.33 mm is also obtained from the pore volume per unit weight of PGP50 of 0.323 cm^3/g and the area receiving sunlight per unit weight of PGP50 of 9.7 cm^2/g ((0.323 cm^3/g) / (9.7 cm^2/g) = 0.33 mm).

Because the effective light-pass length of PGP50 is 33% of the thickness of PGP50, the self-light-shielding effect of $Ru(bpy)_3^{2+}$ is mitigated to 33% of $Ru(bpy)_3^{2+}$ concentration in nanopores. Thus, the effects when light-pass length is shorter, is obtained by using porous glass plate.[4]

The accumulation rate of $MV^{\bullet+}$ of solution system containing 1.6-3.1 mM $Ru(bpy)_3^{2+}$ and 3 mM MV^{2+} was about 49-66% of solution system containing 0.5 mM

$Ru(bpy)_3^{2+}$ and 3 mM MV^{2+} by the self-light-shielding effect of $Ru(bpy)_3^{2+}$ (data not shown). On the other hand, the accumulation efficiencies of $MV^{\bullet+}$ with respect to photon flux density for the PGP50 system was about 67% of the solution system containing 0.5 mM $Ru(bpy)_3^{2+}$ and 3 mM MV^{2+} (Figure 3 in text). The rate of photoreaction achieved inside PGP50 was higher than that of the solution system with similar self-light-shielding effect. This result seems to be obtained by not only mitigation of the self-light-shielding effect using PGP50, but also condensation of MV^{2+} in nanopores.

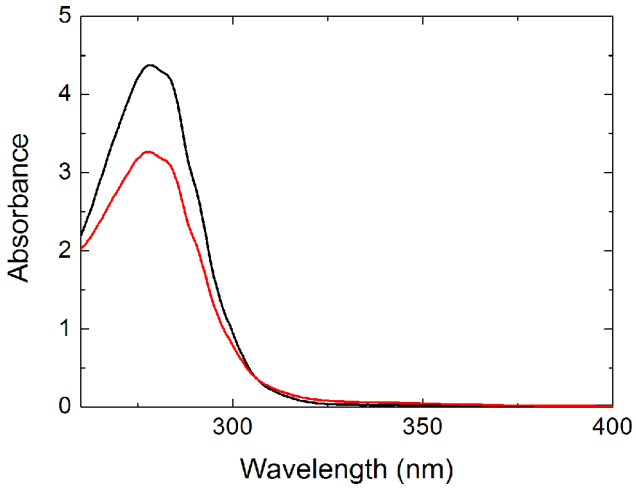

Figure S1. Estimation of the amount of FDHadsorbed in PGP50 (thickness: 1 mm). Dilution factor-corrected absorption spectra of FDH solutions before (black line) and after soaking PGP50 (red line). The soaking solution (25 mM MES-NaOH, pH 6.6) contained 41 μM FDH. The spectra were acquired using a quartz cell with an optical path length of 10 mm.

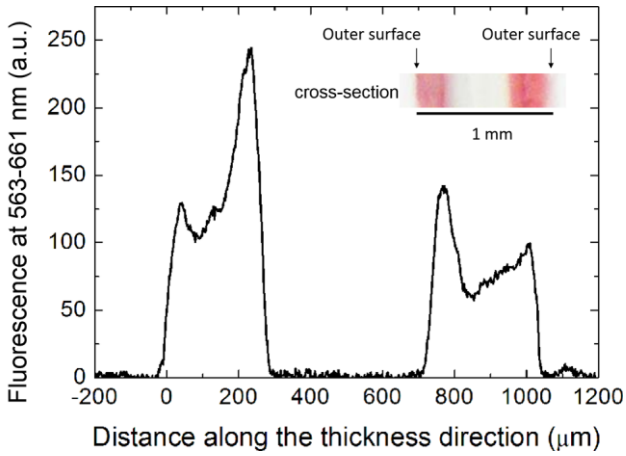

Figure S2. Distribution of rhodamine-labeled formate dehydrogenase (Rh-FDH) inside PGP50 (thickness: 1.0 mm). The fluorescence intensity at 563–661 nm was detected with a confocal laser scanning microscope by x-scanning along the thickness direction of PGP. The black line represents the raw fluorescence intensity profile. The amount of Rh-FDH adsorbed inside PGP50 was 35 nmol/g PGP50. The fluorescence spectra inside Rh-FDH/PGP50 measured at 0, 140, and 240 μm from the surface are shown in Figure S3. The insets shows a photograph of a cross-section of Rh-FDH/PGP50. Rh-FDH (pink) was preferentially adsorbed within a depth of ~0.3 mm from the surfaces of PGP50.

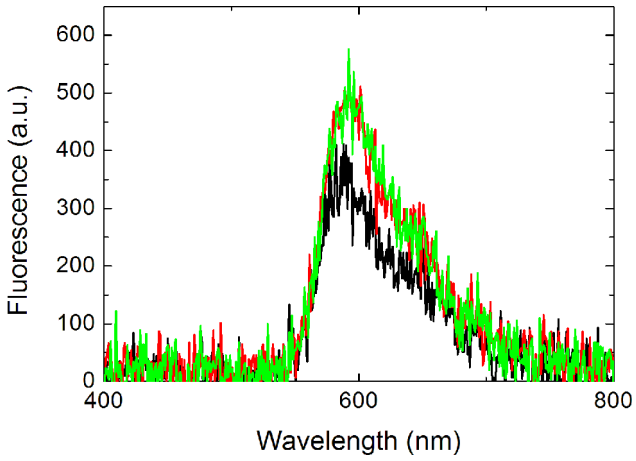

Figure S3. The fluorescence spectra measured at 0 (black), 140 (red), and 240 μm (green) from the surface inside Rh-FDH/PGP50.

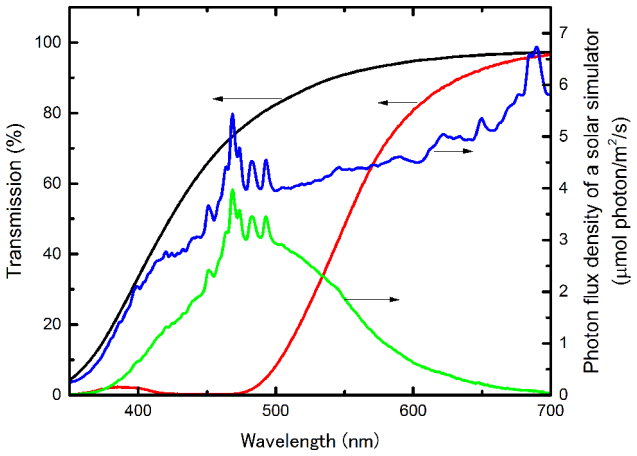

Figure S4. Transmittance spectra of PGP50 (black trace) and $Ru(bpy)_3^{2+}/MV^{2+}$/PGP50 (red trace) immersed in a solution. The thickness of PGP50 was 1 mm. The photon flux density of a solar simulator used in this work (YSS-E40, Yamasita Denso, Tokyo, Japan) is shown as a blue trace. The photon flux density absorbed by $Ru(bpy)_3^{2+}/MV^{2+}$/PGP50 is shown as a green trace.

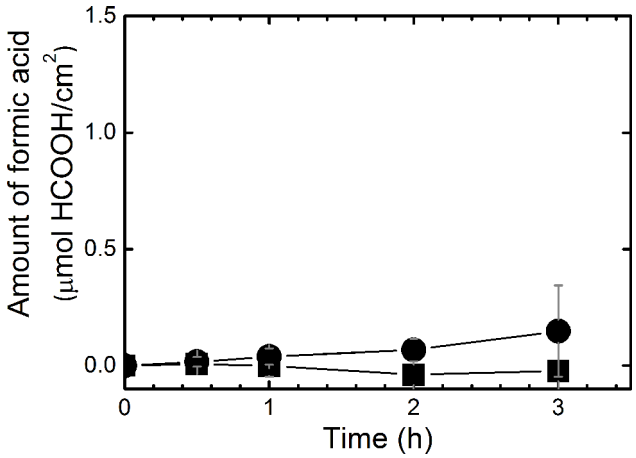

Figure S5. Time evolution of light-induced formic acid production by $Ru(bpy)_3^{2+}/MV^{2+}$/FDH/PGP50 (●) in 0.1 M MES-NaOH (pH 6.6), 20 mM EDTA without $NaHCO_3$ and the $Ru(bpy)_3^{2+}/MV^{2+}$/FDH solution (■) consisting 0.1 M MES-NaOH (pH 6.6), 20 mM EDTA, 0.5 mM $Ru(bpy)_3^{2+}$, 3 mM MV^{2+}, and 41 μM FDH without $NaHCO_3$. The amounts of $Ru(bpy)_3^{2+}$, MV^{2+}, and FDH inside PGP50 are described in the text.

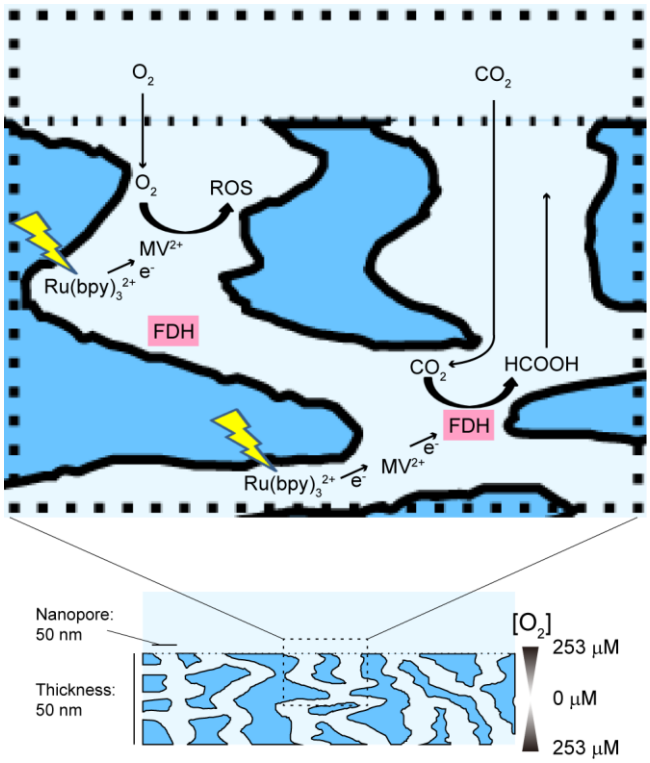

Figure S6. Proposed enhancement mechanism of the CO_2 photoreduction rate of $Ru(bpy)_3^{2+}/MV^{2+}$/FDH/PGP50. Because $MV^{\bullet+}$at the both sides of the plate reduce oxygen to reactive oxygen species (ROS), oxygen concentration in the central region inside PGP is significantly low. CO_2 photoreduction is mainly occurred by photoreactions in the central region inside PGP.

REFERENCES

(1) Tanaka, H.; Yazawa, T.; Eguchi, K.; Nagasawa, H.; Matsuda, N.; Einishi, T. Precipitation of Colloidal Silica and Pore Size Distribution in High Silica Porous Glass. *J. Non-Cryst. Solids* **1984**, *65*, 301-309.

(2) Yazawa, T.; Tanaka, H.; Eguchi, K.; Yokoyama, S. Novel Alkali-Resistant Porous Glass Prepared from a Mother Glass Based on the SiO2–B2O3–RO–ZrO2 (R=Mg, Ca, Sr, Ba and Zn). *J. Mater. Sci.* **1994**, *29*, 3433-3440.

(3) Noji, T.; Kondo, M.; Jin, T.; Yazawa, T.; Osuka, H.; Higuchi, Y.; Nango, M.; Itoh, S.; Dewa, T. Light-Driven Hydrogen Production by Hydrogenases and a Ru-Complex inside a Nanoporous Glass Plate under Aerobic External Conditions. *J. Phys. Chem. Lett*. **2014**, *5*, 2402-2407.

(4) Noji, T.; Kawakami, K.; Shen, J.-R.; Dewa, T.; Nango, M.; Kamiya, N.; Itoh, S.; Jin, T. Oxygen-Evolving Porous Glass Plates Containing the Photosynthetic Photosystem II Pigment–Protein Complex. *Langmuir* **2016**, *32*, 7796-7805.